In-plane Strains Measurement by Using the Electronic Speckle Pattern Interferometry

Koung-Suk Kim*, Hyun-Chul Jung*, Ki-Soo Kang*, Jong-Kook Lee, Soon-Suck Jang*** and Chung-Ki Hong******

(*Received April 8, 1997*)

Two-dimensional in-plane displacements and strains are measured using an electronic speckle pattern interferometry (ESPI) system based on the dual beam speckle interferometric method. Different types of specimens are used: a flat plate, a cracked-plate, and plate with a central hole of 12 mm diameter. Two-dimensional fringes obtained from real-time images are analyzed by an image analyser. The values of in-plane strains obtained by the ESPI technique show high accuracy compared with those measured by strain gages.

Key Words: Coherent Light, Electronic Speckle Pattern Interferometry (ESPI), Fringe Pattern, Image Processing

1. Introduction

When coherent light, for example, a continuous wave (CW) of Ar-laser is illuminated on an optically rough surface, the irregularity of the surface produces random self-interference patterns of light. If the pattern image is viewed by a lens, it would consist of bright and dark spots with a grainy speckle pattern. Speckle interferometry is defined as the generation of moire fringes which result from the subtraction between a pair of random speckle patterns obtained before and after the deformation of an object. The fringes are produced by the relative phase difference caused by the deformation.

The speckle interferometric technique is suitable for the measurement of both out-of-plane and in-plane displacements, especially for complex motions of an object. Speckle patterns generated before and after the deformation of an object produce fringe pattern images which represent the contour lines of phase differences caused by surface displacements. According to the ESPI process, the image of the reference object is first recorded on a frame grabber, and then the image of the deformed live object is electronically subtracted from that of reference object. The subtracted image with fringe pattern is displayed on a monitor in real-time at a speed of 30 frames/sec. This monitoring is used to visualize strain fields and to measure in-plane displacements. Contrary to other optical techniques—Moire or Photoelastic coating method—the ESPI method is a non-contacting technique and does not require any preprocessing of the specimen surface. In this study, we measure two-dimensional in-plane displacements and strains using the ESPI technique and CCD camera combined with an image processing system. We also compare the values obtained by the ESPI method with those measured by a strain gage.

* Department of Mechanical design Engineering, Chosun Uniyersity, Kwangju, 501-759.
** Department of Materials Engineering, Chosun University, Kwangju, 501-759.
*** Department of Control and Measurement Engineering, Chosun University, Kwangju, 501-759.
**** Department of Physics, Pohang Institute of Science and Technology, Pohang, Korea, 790-784.

2. Basic Principles

2.1 Speckle pattern interferometry (SPI)

High coherent laser light has made it possible to observe the interference effects of scattered lights from a rough surface. In the case of speckle patterns observed at distance greater than the diameter of the illuminating beam as shown in

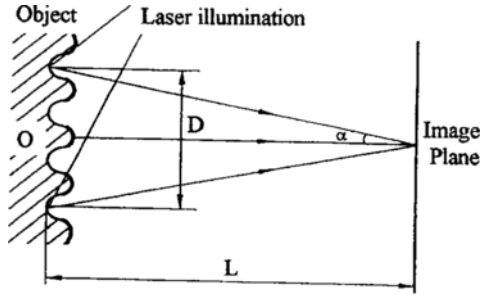

(a) Objective speckle pattern

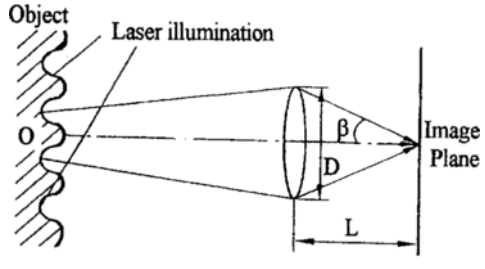

(b) Subjective speckle pattern

Fig. 1 The basic optical system.

Fig. 1(a), these speckles are called objective speckle. Whereas, the speckles appeared by imaging lens of a laser-illuminated object, are called subjective speckle, as shown in Fig. 1(b).

In the case of objective speckle, the speckle size σ_o is given as follows;

$\sigma_o=1.22(\lambda L/D)$, where λ is the laser wavelength, L is image distance, and D is the diameter of the laser illumination beam. In the case of the subjective speckle, the speckle size is given by $\sigma_s=1.2(1+M)\lambda F$ in terms of the f-number F (ratio of the focal length to

the diameter of imaging lens) and the magnification M of the imaging lens. In order to measure in-plane displacements, we design the experimental setup based on the dual-beam interferometer as shown in Fig. 2.

The two object surfaces are symmetrically oriented with respect to the z-direction at an equal collimated, coherent laser beams illuminating angle.

The speckle patterns formed from scattered light at equal angles θ are superimposed to produce a new speckle pattern before object

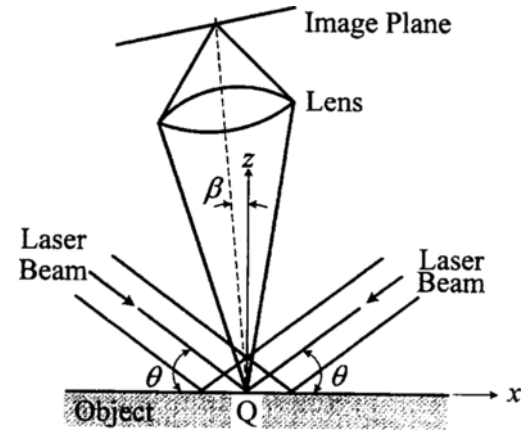

Fig. 2 The basic optical system of the dual-beam speckle pattern interferometric method for measuring in-plane displacement.

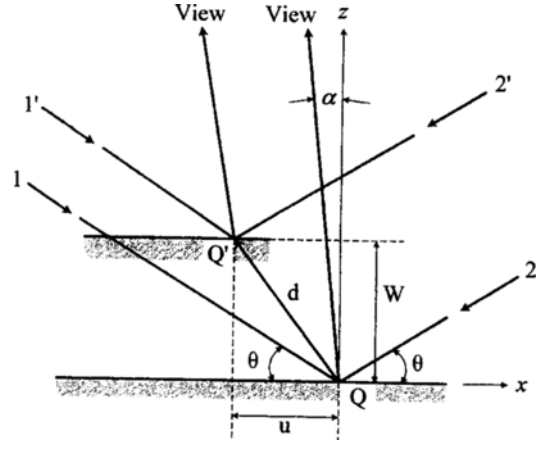

Fig. 3 Relationship between the displacement and optical length change.

deformation. If any displacements occurr in the x-direction, these will give rise to a change in the optical path length. Eventually the two independent coherent speckle patterns are no longer of the same phase. Therefore, the speckle pattern before deformation is compared with that after deformation by an image processor. In this case, laser beam 1 is regarded as a reference for beam 2, or vice versa. Consider any displacements at a point Q as in Fig. 3. Let L_1 and L_2 be the changes of the optical path length in beams 1 and 2 to the viewing direction respectively. Then the change of optical path length L_1 is given as follows;

$$L_1 = u\cos\theta + w\sin\theta + w\cos\alpha + u\sin\alpha \quad (1)$$

likewise for the path change L_2

$$L_2 = w\cos\alpha + u\sin\alpha - u\cos\theta + w\sin\theta \quad (2)$$

Since one illumination beam acts as a reference beam for the other, the next path change between the two beams due to the x-direction displacement u is given by

$$L_2 - L_1 = 2u\cos\theta = \Delta L \quad (3)$$

Set the fringe-order number n, in whice case the equation of the fringe field is

$$n\lambda = 2u\cos\theta \rightarrow u = \frac{n\lambda}{2\cos\theta} \quad (4)$$

2.2 Electronic speckle pattern interferometry (ESPI)

The ESPI technique has been used in various fields of optical tests and measurements since its principle was demonstrated by Butters and Leendertz (1972).

In the ESPI method, the lenses and films used in speckle interferometry are replaced by a CCD camera and a TV monitor, and electronic signal processing is utilized to produce the interference fringe patterns. The merit of the ESPI method is that it gains real-time interferometric fringes by displaying on a TV monitor without any photographic processes. A block diagram for the image processing system of this study is described in Fig. 4. As a reference image in 256 gray level, the initial object image before deformation is recorded in the memory by the frame grabber. The image processor then compares the reference image with the live image under deformation as a form of electronic subtraction process. About 1/30 sec is needed to record a single speckle pattern frame.

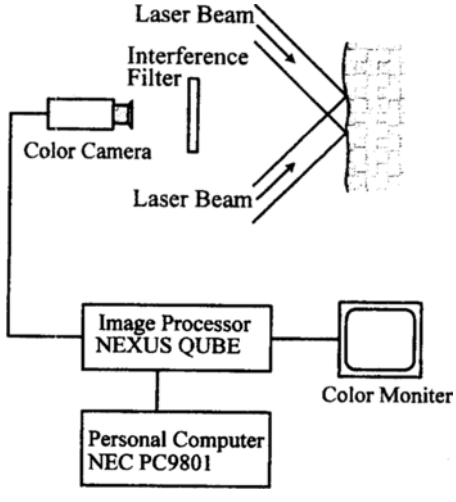

Fig. 4 Block diagrams of image processing system.

That is to say, the average product of two speckle patterns may be performed by a CCD camera and a frame grabber. The fringe changes in relative phase or constant displacement of object are then displayed on the monitor.

However, the displaying image is usually of low quality. For this reason, these fringes are treated by image processing with a series of enhancement, smoothing, thresholding and expansion-contraction, thinning, labeling in sequence for the reduction of speckle noise, and finally the improvement of fringe contrast.

3. Experimental Apparatus and Procedure

The type of image processor and the personal computer used in this study are the NEXUS QUBE and NEC PC-9801, respectively. The

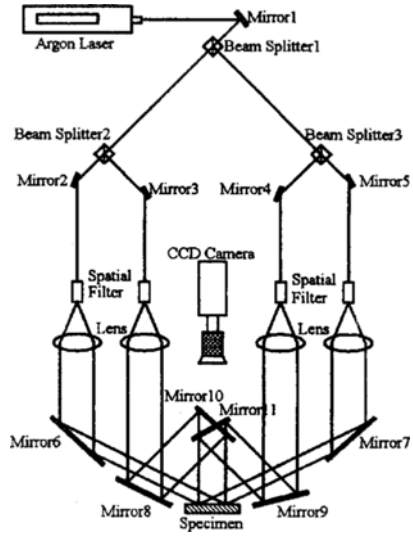

Fig. 5 The experimental optical layout adopted in this experiment for ESPI.

main light source was an argon laser with 200 (mW) continuous-wave operating at a wavelength of 514.5 (nm). Figure 5 shows the optical arrangement based on the dual beam interferometer for measuring the in-plane displacement.

To measure the two dimensional in-plane displacement, mirrors 10 and 11 as seen in Fig. 5 were illuminated toward the upward and the downward surfaces of object, respectively. Mirrors 6 and 7 are employed to illuminate the right and left side of the object, respectively. The specimens used in an uniaxial tensile test consist of three types of plates: a flat plate, cracked-plate, and flat plate with a central hole of 12 mm in diameter. In order to increase the degree of reflection, object surfaces are coated with a white color coating material. To compare the reliability of the ESPI method with the strain gage method, many strain gages of $P_{1\sim5}$, $G_{1\sim3}$ and $C_{1\sim9}$ were attached on the front side of each specimen, as seen in Fig. 6.

To measure and visualize the in-plane displacement of the specimen, a uniaxial tension is loaded by the tension tester, which is composed of the fixed upper part and the lower part with a worm and a wormwheel to put the load upon the specimen in one direction. The given load upon a specimen is detected by a loadcell.

Also, the specimen is attached to the grip with epoxy, bolt and nut. It is important to make uniform load on specimens. This problem is solved by inspecting fringe patterns. If a specimen is off center, by given load, the specimen will be loaded partially. That is, a slanted specimen to one side shows the fringe pattern which leans to one side. Therefore, using bolts on a tension tester, the specimen is adjusted until the fringe pattern is in parallel.

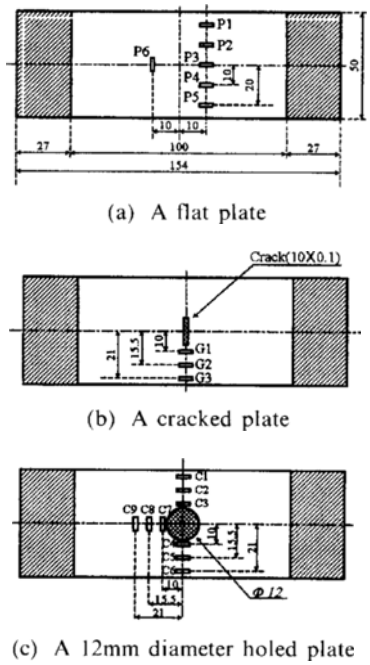

(a) A flat plate

(b) A cracked plate

(c) A 12mm diameter holed plate

Fig. 6 The position of strain gage.

4. Analysis of Interferometric Fringe

4.1 Image processing of original image

The fringe patterns produced on a flat plate, a cracked-plate and a holed-plate by a uniaxial tension are analyzed in both the horizontal and vertical direction for the measurement of in-plane displacement.

But the images of the fringe patterns by ESPI are not clear of contrast and visibility compared with those of the holographic interferometry using smoothing reference beams.

To clear the fringe patterns and remove the speckle noise, a series of image processing operations, such as the enhancement of fringe patterns, smoothing, thresholding, expansion-contraction, thinning, and labeling, are performed and the enhanced fringe image is compared with the original interferometric fringe image as shown in Fig. 7. The distribution of image intensity after enhancement is smoothed as shown in Fig. 8(a).

Fig. 7 Original fringe pattern produced by a uniaxial tension on a cracked specimen.

(a) (b)

Fig. 8 Digital image processing of smoothing, thresholding, expansion and contraction and thinning.

Although the original images may be shown the black- and white-image, the data for the image contains more than three colors. Therefore, it is necessary to convert the multi-values of image data to two values, that is, the white- and black-image data.

For this procedure, a thresholding operation was performed. Also, to remove the unnecessary components of the thresholding image and to detect the central line between fringes, the processing of the expansion-contraction and thinning is performed. Over these procedures, the fringe pattern image was changed from Fig. 8(a) to Fig. 8 (b).

4.2 Strain measurement

Suppose there are two adjacent fringes of n and $n+1$ order fringe, the displacements of each fringes are given by

$$u_n = n\lambda/2 \cos \theta \tag{5}$$

$$u_{n+1} = (n+1)\lambda/2 \cos \theta \tag{6}$$

The difference between two displacements of the adjacent fringes Δu is given to as follows:

$$\Delta u = \lambda/2 \cos \theta \tag{7}$$

As the above equation is applied to a general fringe pattern over the surface in Fig. 9, a normal strain ϵ_x may be interpreted as follows:

$$\epsilon_x = \frac{\Delta u}{F} = \frac{\lambda}{2 \cos \theta F} \tag{8}$$

where F is the fringe spacing.

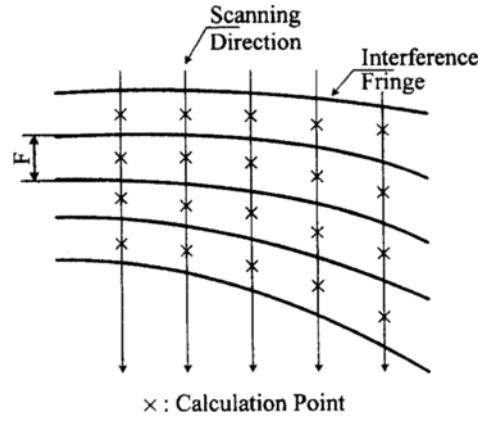

Fig. 9 Calculation of strain from the spacing of two adjoining interference fringes.

4.3 Calculation of theoretical strain and error ratio

In order to compare the experimental values from ESPI with those from the strain gage, we calculate the strain at the position of the gages. By the measurement of strain values at the center of between two fringes calculation point and the first-order interpolation of their spacing, the theoretical strain for a flat plate ε_L is given as follows:

$$\varepsilon_L = P/AE \tag{9}$$

where P is the difference of the load detected by the loadcell, A is the cross area of a flat plate specimen, and E, Young's modulus of the specimen, is 73.88 (GPa). If ε_E is the strain measured by the ESPI method and ε_G is that by the strain gage, the error of ratio(%) between the two methods is given as follows:

$$\text{Error}(\%) = [(\varepsilon_E - \varepsilon_G)/\varepsilon_G] \times 100 \tag{10}$$

5. Results

Table 1 and Fig. 10 show the experimental results of a flat plate. In this table, the loading value is the relative values measured by the loadcell, which is the difference before and after loading. In the case of a flat-plate specimen, the measurement results of strain by the ESPI method agree within the error ratio of 6.5% compared with those measured by the strain gage method.

Table 1 Experimental values of flat plate (P_2-Gage).

Load (N)	Strain ($\times 10^{-6}$)			Error (%)
	Theory	ESPI	Gage	
54.98	37.23	38.13	36	5.92
73.21	49.57	50.58	49	3.22
91.53	61.99	66.52	62	7.29
108.09	73.20	77.86	75	3.81
128.18	86.81	93.73	87	7.74
146.51	99.22	107.59	99	8.68
164.84	111.63	114.63	113	1.63
183.16	124.04	130.03	125	4.02

Table 2 Experimental values of a cracked plate (G_1-Gage).

Load (N)	Strain ($\times 10^{-6}$)		Error (%)
	ESPI	Gage	
32.93	54.23	52	4.29
37.34	42.38	41	3.37
43.90	53.86	56	−3.82
45.77	55.32	53	4.38
47.63	55.15	51	8.14
51.25	58.65	58	1.12
60.47	70.28	73	−3.73
73.21	91.87	91	0.96

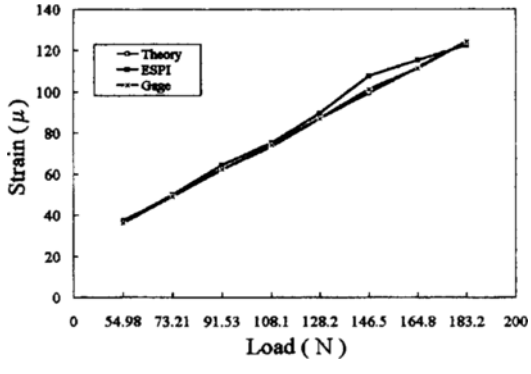

Fig. 10 Comparison of the experimental results of ESPI with those of strain gage and theoretical values on a flat plate (P_2-gage).

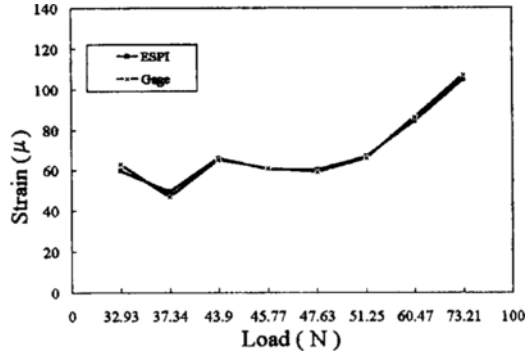

Fig. 11 Comparison of the experimental results of ESPI with those of strain gage on a cracked plate (G_1-gage).

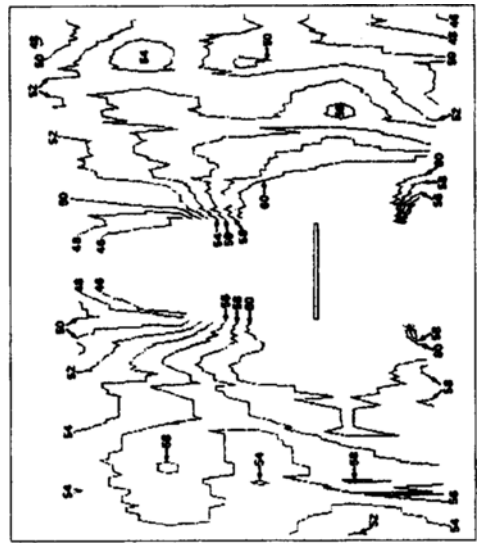

Fig. 12 Strain distribution of a cracked plate subjected to uniaxial tension (73.21 N).

Similarly, for a cracked-plate, the experimental results measured by a G1-gage is also presented in Table 2 and Fig. 11.

For a cracked-plate, the error ratio was within ±5% in comparison with the measurements of strain gages $G_1 \sim G_3$ attached on the front side of the specimen.

Also, observed in the horizontal illumination, the strain distribution for a cracked-specimen under a uniaxial tension is shown in Fig. 12. In this figure, the distribution line is described by connecting each strain values (ε_{yy}) calculated at each scanning directions. The results of the holed

Table 3 Experimental values of a circular holed plate (C_4-Gage).

Load (N)	Strain ($\times 10^{-6}$)		Error (%)
	ESPI	Gage	
78.09	70.43	68	3.57
91.63	90.66	86	5.41
109.97	108.56	105	3.39
128.31	126.71	121	4.71
146.66	154.58	151	2.34

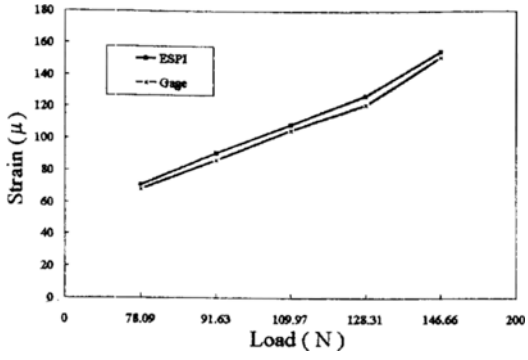

Fig. 13 Comparison of the experimental results of ESPI with those of strain gage on a cracked plate (C_4-Gage).

Fig. 14 Strain distribution passed through the image processing in subjection to uniaxial tension (146.66 N).

-specimen are shown in Fig. 13 and Table 3. Also, Fig. 14, showing the strain distribution as predicted by the conventional theory, indicates that the strain concentration occurs around the hole. The fringe spacing is in inverse proportion to the in-plane displacement (μ) created by the uniaxial tension, and the fringe orientation due to the strain distribution is perpendicular to the object displacement as shown in Figs. 12 and 14.

6. Conclusions

The in-plane strain and the strain distribution on three types of specimens (a flat-plate, a cracked-plate, and a holed-plate) were measured using the ESPI technique under uniaxial tension. The values of in-plane strains obtained by the technique show high accuracy compared with those measured by strain gages. It is suitable to measure the in-plane displacements of an object in real-time and possible to measure out-of -plane displacements by modifying the speckle interferometer configuration.

In a flat-plate, the errors of results measured by the ESPI method are within an error ratio of 6.5% compared with those measured by the strain gages. For a cracked-plate, the error ratio was within $\pm 5\%$ compared with the values measured by the strain gages attached on the front side of the specimen. The strain concentration in cracked and holed specimens is shown to occur at the edges of a crack or a hole.

Acknowledgements

This study was supported by the Korea Science and Engineering Foundation (KOSEF) (No. 95 -0200-03-3).

References

Butters, J. N. and Leendertz, J. A., 1972, "Application of Video Techniques and Speckle Pattern Interferometry to Engineering Measurement," *Proc. Symp. of Eng. Appl. of Holography*, Society of Photo-optical Instrum. Eng., pp. 361～375.

Denby, D. and Leendertz, J. A., 1974, "Plane -Surface Strain Examination by Speckle-Pattern Interferometry Using Electronic Processing," *J. Strain Analysis*, Vol. 9, No. 1, pp. 17~25.

Develis, J. B., 1967, *Theory and Applications of Holography*, Addison-Wesley, Tokyo, p. 155.

Ennos, A. E., 1968, "Measurement of In-plane Surface Strain by Hologram Interferometry," *J. Phys. E Sci. Instrum.*, Vol. 1, Ser. 2, pp. 731 ~734.

Erf, R. K., 1974, *Holographic Nondestructive Testing*, Academic Press, p. 87.

Hung, Y. Y. and Taylor, C. E., 1975, "Measurement of Surface-Displacements Normal to Line of Sight by Holo-Moir Interferometry," *J. Appl. Mech*, Vol. 42, No. 1, pp. 1~4.

Jones, R. and Wykes, C., 1989, *Holographic and Speckle Interferometry*, Cambridge University Press, London, p. 90.

Leendertz, J. A., 1970, "Interferometric Displacement Measurement on Scattering Surface Utilizing Speckle Effect," *J. Phys. E*, Vol. 3, No. 3, pp. 214~218.

Martin, D. J. V., 1976, *Material Evaluation*, 36 p. 53.

Schumann, W. and Dubas, M., 1979, *Holographic Interferometry*, Springer-Verlag, p. 77.

Schumann, W., Zurcher, J. P. and Cuche, D., 1985, *Holography and Deformation Analysis*, Springer-Verlag, Berlin, p. 151.

Smith, H. M., 1975, *Principles of Holography*, 2nd ed., John Wiley & Sons, Tokyo, p. 98.

Sumi, S., 1976, "Speckle Correlation Method for Measurement of Surface Structural Changes Caused by Fatigue," *Proc. 19th Japan Congr. Material Research*, Tokyo, pp. 17~21.